Journal of the Southeastern Association for Research in Astronomy, **5**, 8-11, 2012 February 1

MODELING THE VARIATION OF X-RAYS FROM WOLF-RAYET STARS

Michael McFall[1]
Department of Physics and Astronomy, Butler University, IN, 46208

and

Richard Ignace
Department of Physics and Astronomy, East Tennessee State University, TN, 37614

ABSTRACT

Wolf-Rayet (WR) stars are massive stars with powerful, x-ray-emitting winds. Some single stars have been observed to have a periodic behavior. A model using a spiral structure in the winds has been created to explain what causes this variability. We used this model to examine the possibility of x-ray variation in single WR stars. We have then used the model to determine probabilities of finding previously unknown variation in the x-rays of single WR stars given a set of parameters that define the spiral structure and the properties of the wind.

Subject headings: X-ray stars

1. INTRODUCTION

Wolf-Rayet stars are OB-stars of 10-25 $M_\odot$ (Crowther 2007) that have evolved off the main sequence and have lost their outer envelopes. This is evident from the strong helium emission lines and the absence of hydrogen lines that are observed (van der Hucht 2006). The winds of WR stars have velocities of 1500-2500 km s^{-1}. The main mechanism driving these winds is transfer of momentum from photons to the stellar atmosphere through spectral line absorption (Crowther 2007). WR stars have very high mass loss rates of about $10^{-5}M_\odot$ yr^{-1}.

The driving mechanism of the winds can be unstable which causes portions of the wind to accelerate faster than others to create shocks in the winds (Gayley & Owocki 1995). These shocks convert mechanical energy into thermal energy causing portions of the winds to reach temperatures in the millions of Kelvin which is hot enough to emit x-rays. The luminosity of the x-rays is much less than the total luminosity of the star, at about $10^{-7}L_\star$.

Many WR stars have been observed with a periodic variability in their optical spectrum. Some of these are binaries and the variations are caused by structures formed from the colliding winds. Figure 1 shows an infrared image of WR104, a binary system, which has a spiral structure from the interaction of the two winds. Others are thought to be single stars with structured winds. We looked into whether a structured wind would cause an observable variation in the x-ray component. To describe what causes these single stars to be periodic, we have modeled a structure in the wind that can either produce more or less x-rays than to the rest of the wind.

In §2 we introduce our model for x-ray production and the geometry for the wind structure. In §3 synthetic data extracted from the model and results are given. In §4 we summarize our model and make conclusions about the detectability of x-ray variation.

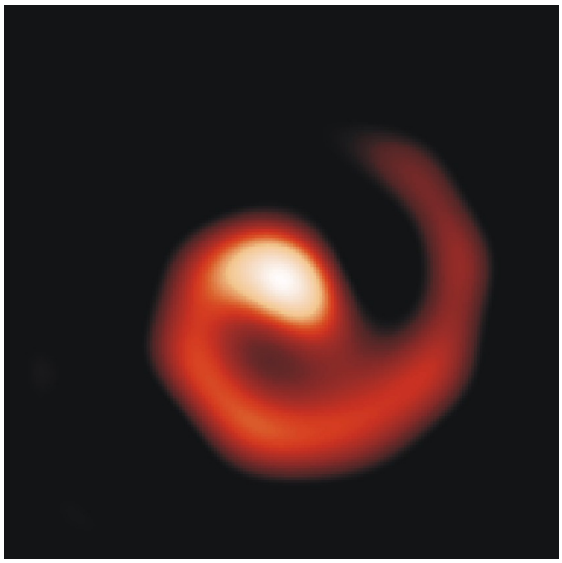

Fig. 1.— This is a picture of WR104 which is in a binary, but has a spiral structure similar to the structure used in the model. (Photo Credit: U.C. Berkeley Space Sciences Laboratory/W.M. Keck Observatory)

2. MODEL

2.1. *Spherically Symmetric Wind*

Before discussing a structured wind, it is useful to introduce our model for the production of x-rays that occur in spherically symmetric winds. The amount of x-ray production depends only on radius in a wind with density having the form used in Ignace, Oskinova,& Foullon (2000):

$$\rho(r) = \rho_0 \frac{v_\infty R_\star^2}{v(r) r^2}, \tag{1}$$

$$v(r) = v_\infty \left(1 - b\frac{R_\star}{r}\right)^\beta, \tag{2}$$

where $R_\star$ is the radius of the star, r is the distance from the star's center, and v_∞ is the terminal velocity of the wind. The β used in the velocity law is a parameter of

Electronic address: mmcfall@butler.edu
[1] Southeastern Association for Research in Astronomy (SARA) NSF-REU Summer Intern
[2] Visiting observer, SARA Observatory at Kitt Peak, Arizona, which is operated by the Southeastern Association for Research in Astronomy

the wind that determines how fast the wind reaches v_∞ and was set to 1 as is typical of early hot star winds (Pauldrach, Puls, & Kudritzki 1986). The variable b is a parameter of the initial wind velocity with a value of $b = 1 - v_0/v_\infty$. To calculate the luminosity of the x-rays that would be observed we used the equation from Ignace et al. (2000):

$$L_x(E) = \int_0^{2\pi} \int_0^{\pi} \int_{R_\star}^{\infty} \frac{1}{4\pi} \Lambda(E) \rho^2(r) e^{-\tau(E,r,\theta_\star,\phi_\star)} \, dV, \tag{3}$$

where r, $\theta_\star$, $\phi_\star$ are spherical coordinates of the star, Λ is the cooling function that is a power law over the energies concerned, and τ is the optical depth factor. While this integral does converge, it is more convenient computationally to use the substitution $u = R_\star/r$.

As the x-rays travel through the wind some of them are absorbed. The amount of x-rays seen by a distant observer from a certain radius in the winds is determined by the optical depth factor,

$$\tau = \int_z^{\infty} \kappa \rho(r) dz. \tag{4}$$

Photo-absorption by inner K-shell ionization causes κ to follow a power law in energy (Cox 2000). Using the power law and the density law we arrive at the following equation for optical depth:

$$\tau(E, p, z) = T_0 \left(\frac{E}{E_0} \right)^{-Q} \int_z^{\prime\infty} \frac{1}{(1 - bu)^\beta} \frac{dz}{p^2 + z^2}, \tag{5}$$

where p and z are the cylindrical coordinates of the observer and T_0 determines the radius where the wind becomes optically thin. A T_0 of 0 means all x-rays will escape from the wind. At higher values the x-rays produced near the star are more strongly absorbed and the observed x-rays emerge from farther out in the wind. The value of Q is set to 2.3 because it is a typical value for the interstellar medium (Cox 2000) and appropriate for OB star winds (Ignace et al. 2000). The value of E_0 was set to 1keV as it is a convenient fiducial for the energy. Using the relationship $z = p \tan(\theta)$, along with $u = R_\star \sin(\theta)/p$, where θ is the angle between the radial line to the point where the optical depth is being calculated and the line of sight, we transformed the previous equation into the following one:

$$\tau = T_0 \left(\frac{E}{E_0} \right)^{-Q} \int_0^{\theta} \frac{d\theta}{[p - bR_\star \sin(\theta)]} \tag{6}$$

which has different analytic solutions depending on the value of the impact parameter, p.

2.2. *Wind with Spiral Structure*

In a wind containing a structure, the model for x-ray emission and absorption is nearly identical to that in a spherically symmetric wind. The only difference being that the structure does not produce the same amount of x-rays as the rest of the wind. The structure used in our phenomenological model is a spiral shape about the equator of the star. Using the velocity equation defined earlier and $v_\phi = v_{rot} R/r$, the equation of motion for the guiding center of the spiral as given by Ignace, R., Hubrig, S., & Schöller, M. is:

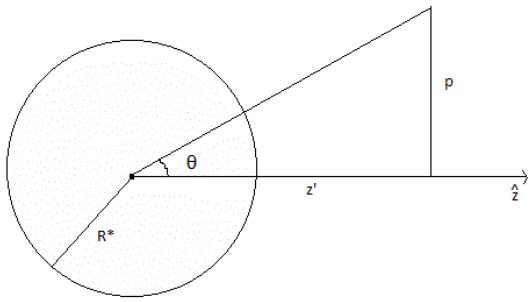

FIG. 2.— Geometry being used in optical depth integral.

$$\phi(t, u) = \Omega \cdot (t - t_0) - \frac{v_{rot}}{v_\infty} \cdot \left[\frac{1 - u}{u} + b \ln\left(\frac{w(u)}{w_0 u} \right) - \frac{1}{b} \ln\left(\frac{w(u)}{w_0} \right) \right] \tag{7}$$

where v_{rot} is the rotation velocity of the star, $w(u) = v(u)/v_\infty$, and $w_0 = w(1)$. The phase of the spiral, ψ, is the decimal portion when $\Omega \cdot (t - t_0)$ is divided by the period of rotation, P. The spiral structure is modeled as a cone with a constant opening angle that has its center on the spiral equation above. We assumed a deficit of x-ray emissions from the spiral to cause the variability in x-ray luminosity caused by a difference in the amount of x-ray producing gases. We multiplied the luminosity equation by an emissivity factor, e, at each point. If the point was outside the spiral e was set to 1 and if it was inside e was set to another number. We used values of e inside the spiral between 0 and 1. Values above 1 also cause variabilty but give similar light curves as those between 0 and 1 so are not discussed here.

3. MODELED DATA & RESULTS

By integrating the emissivity over the whole wind and plotting it against energy, we create a synthetic spectrum as shown in figure 3. A peak is seen in the spectrum which is caused by the power law in $e^{-\tau}$ dominating Λ at small values of E/E_0. The area under the curve is representative of the number of counts observed. When the phase is changed, the spiral moves around the star making a different part occulted by the star thus changing the luminosity.

Each point on the light curve is generated by integrating the area under a spectrum at the apppropriate phase. The model was run to show the dependence of the shape of the light curve on various parameters. To see the effects better, we normalized each one by dividing each curve by its highest value. The results of these runs with v_{rot} = 40 km s^{-1} and v_∞ = 1700 km s^{-1} e.g., (Chené & St-Louis 2010) are in figure 4. Shown are the effects of changing the three main parameters that affect the shape of the light curve: emissivity, e; opening angle, γ; and inclination of the rotation axis to the line of sight, i.

To simulate real data that would be collected, we have added noise to each spectrum. We assumed that the amount of noise would be less than or equal to the accounted error in measurement of the number of counts of each energy bin, $\sqrt{C}$. To add noise we added a random

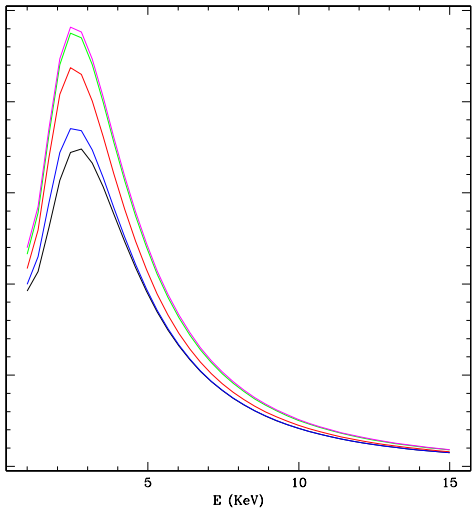

FIG. 3.— Plot of spectra at various phases with $T_0 = 3$. The y-axis is representative of counts, but has no definite scale

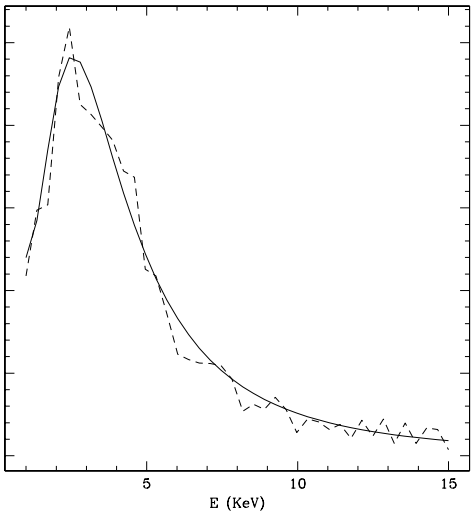

FIG. 5.— This is a plot of a theoretical spectrum (solid line) and of the same spectrum with noise added (dashed line), with a value of $T_0 = 3$

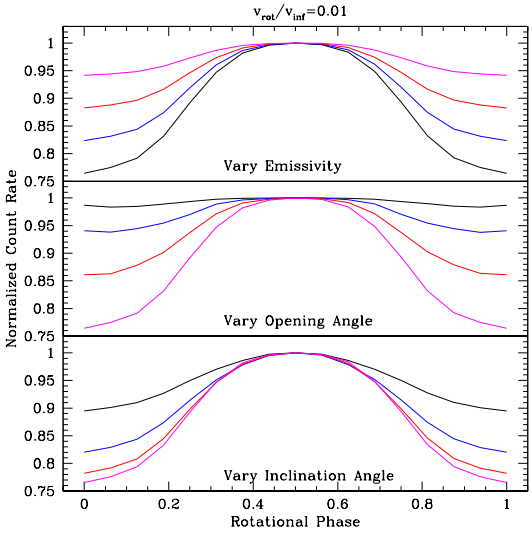

FIG. 4.— Model results for x-ray variability with phases *Top Panel*: The emissivity, e, of the spiral as a percent of the value of the rest of the wind is changed to 0%-black, 25%-blue, 50%-red, and 75%-magenta. *Middle Panel*: The opening angle, γ, is changed in degrees to 10-black, 20-blue, 30-red, and 40-magenta. *Bottom Panel*: The inclination angle, i, is changed in degrees to 20-black, 40-blue, 60-red, and 80-magenta. If the value was not being changed it was e=0, γ=40, and i=90.

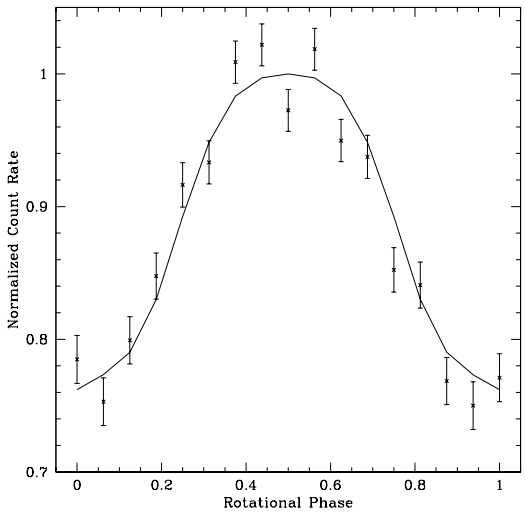

FIG. 6.— This is a plot of a theoretical light curve and of the same light curve points with noise added and showing errors. $T_0 = 3$

value of x where $-\sqrt{C} \leq x \leq \sqrt{C}$. We kept values from becoming negative by scaling each bin so that the total number of counts in the spectrum would be 4000 and returning it to its original value after adding the noise. Scaling to 4000 was chosen because it is a typical value expected from planned future observations of WR6. Figures 5 & 6 show theoretical plots and plots with noise.

3.1. *Detecting X-ray Variable WR Stars*

Noise in the data changes the shape of the light curve and the ability to detect variations. We used the model to determine the probability of detecting x-ray variation of a WR star with a prescribed set of parameters: e, γ, and i. We ran the model one hundred times with sixteen randomly sampled phases each time for a set of parameters. After creating the light curves and adding noise, we calculated the mean using:

$$\bar{N} = \frac{\sum_{i=1}^{16} N_i/\delta N_i^2}{\sum_{i=1}^{16} 1/\delta N_i^2} \tag{8}$$

where N is the total number of counts at each phase and $\delta N_i = \sqrt{N_i}$. We then found the reduced chi squared of fitting the light curve to a flat line with a value equal to $\bar{N}$. A $\chi^2_{red} \geq 3$ likely shows a statistical deviation from being constant. The results are given in Table 1. The table shows the number of occurances for which a particular χ^2_{red} happened out of 100 trials. The default values of e, γ, and i were set to 0%, 40°, and 90° respectively. The first column names the only variable that was changed and what it was changed to.

TABLE 1
DETECTABILITY

Parameter	χ^2_{red}=1	χ^2_{red}=2	χ^2_{red}=3	χ^2_{red}=4	χ^2_{red}=5	χ^2_{red}=6	χ^2_{red}=7	χ^2_{red}=8	χ^2_{red}=9	χ^2_{red}=10
Default[a]	0	0	0	0	2	0	1	3	5	5
e = 0.2	0	0	0	2	10	13	29	20	12	6
e = 0.4	0	4	14	37	31	14	0	0	0	0
e = 0.5	0	20	56	24	0	0	0	0	0	0
e = 0.6	12	67	21	0	0	0	0	0	0	0
$\gamma = 20$	58	42	0	0	0	0	0	0	0	0
$\gamma = 25$	0	37	50	13	0	0	0	0	0	0
$\gamma = 30$	0	3	8	24	34	23	8	0	0	0
$\gamma = 35$	0	0	0	0	5	16	20	17	14	17
i = 20	77	23	0	0	0	0	0	0	0	0
i = 30	1	19	55	25	0	0	0	0	0	0
i = 40	0	0	2	14	37	33	12	2	0	0
i = 60	0	0	1	2	5	5	11	14	20	12

NOTE. — 100 runs were made, varying only one parameter at a time from the default value. Rows not adding to 100 have runs with $\chi^2_{red} > 10$.

[1]Default parameters are e=0%, γ=40, and i=90.

4. CONCLUSIONS

We have constructed a model to determine if it is possible to detect variability in the x-rays of single WR stars that have a known periodic variation in optical wavelengths. We used an equatorial spiral structure in the winds that was dimmer in x-rays than the rest of the wind. It was determined that it is possible to detect such x-ray fluctuations given the expected signal to noise with 4000 counts.

We added simulated noise to the theoretical data to emulate real data. This was shown to affect the ability to determine if a source is varying significantly from the mean. Using $\chi^2_{red} = 3$ means that there is a 99% chance that the source is not constant, we have determined minimum values for the three main parameters that affect the shape of the light curve: e, γ, and i. Variation in the x-ray luminosity is likely to be detected if the spiral is emitting less than 50% of the x-rays or the normal wind. It is probable to detect variation if the operning angle is more than 25°. When the inclination angle is more than 30°, it the variation most likely will be detected.

This project was funded by the National Science Foundation Research Experiences for Undergraduates (REU) program through grant NSF AST-1004872.

REFERENCES

Chené, A.-N., & St-Louis, N. 2010, ApJ, 716, 929
Cox, A. N. 2000, Allen's Astrophysical Quantities,
Crowther, P. A. 2007, ARA&A, 45, 177
Gayley, K. G., & Owocki, S. P. 1995, ApJ, 446, 801
Ignace, R., Oskinova, L. M., & Foullon, C. 2000, MNRAS, 318, 214
Ignace, R., Hubrig, S., & Schöller, M. 2009, AJ, 137, 3339
Pauldrach, A., Puls, J., & Kudritzki, R. P. 1986, A&A, 164, 86
van der Hucht, K. A. 2006, A&A, 458, 453